High electrical conductivity of layered cobalt oxide $Ca_3Co_4O_9$ epitaxial films grown by topotactic ion-exchange method

Kenji Sugiura and Hiromichi Ohta[a)]
Graduate School of Engineering, Nagoya University, Furo-cho, Chikusa, Nagoya 464-8603, Japan

Kenji Nomura, Masahiro Hirano, and Hideo Hosono
ERATO-SORST, JST, Frontier Collaborative Research Center, Mailbox S2-13, Tokyo Institute of Technology, 4259 Nagatsuta, Midori, Yokohama 226-8503, Japan

Kunihito Koumoto[a),b)]
Graduate School of Engineering, Nagoya University, Furo-cho, Chikusa, Nagoya 464-8603, Japan

(Received 1 March 2006; accepted 17 June 2006; published online 21 July 2006)

Epitaxial film of a layered cobalt oxide, $Ca_3Co_4O_9$, was fabricated on a (0001) face of an α-Al_2O_3 substrate by a topotactic ion-exchange method using a γ-$Na_{0.8}CoO_2$ epitaxial film as a precursor. High-resolution x-ray diffraction and atomic force microscope measurements revealed that the film was high-quality (001)-oriented $Ca_3Co_4O_9$ with stepped and terraced surface morphology. The film exhibits a high electrical conductivity of 2.95×10^2 S cm^{-1} and a large Seebeck coefficient of $\sim+125$ μV K^{-1}, which leads to the thermoelectric power factor (TPF) of 4.5×10^{-4} W m^{-1} K^{-2} at 300 K, potentially usable as a building block of the multilayered film structure with an enhanced TPF value. © *2006 American Institute of Physics*.
[DOI: 10.1063/1.2234277]

Thermoelectric energy conversion (TE) is an emerging technology for power generation in the next generation. It may economically utilize waste heat energy thrown away from various industrial factories, transportation system, offices, and home. The performance of TE materials is generally characterized by the dimensionless figure of merit ZT ($=S^2\sigma T/\kappa$, where S, σ, T, and κ are the Seebeck coefficient, electrical conductivity, absolute temperature, and thermal conductivity, respectively).

Recently, p-type layered cobalt oxides, including γ-Na_xCoO_2 ($x\sim0.7$),[1,2] γ-Sr_xCoO_2 ($x\sim0.35$),[3,4] and $Ca_3Co_4O_9$,[5,6] have attracted much attention toward the realization of oxide TE devices[7] because of their good TE performance and advantages over conventional intermetallic alloys of Bi_2Te_3/Sb_2Te_3 (Ref. 8) in terms of thermal stability at high temperature and low toxicity. $Ca_3Co_4O_9$, which exhibits good thermal stability at 1000 K in air, is regarded as a most promising material among the layered cobalt oxides, and hence intensive studies have been made in TE properties of $Ca_3Co_4O_9$ to date.[5–7,9–11] However, the obtained TE performance ($ZT_{300\ K}\sim0.08$) is not good enough for the practical applications because it does not satisfy the ZT value over ~2, which is a generally accepted requirement for the practical TE materials.

In order to further improve the TE performance of $Ca_3Co_4O_9$ for the practical applications, nanostructural design compatible with the intrinsic TE properties of $Ca_3Co_4O_9$ is one of the innovative approaches. Since a high-quality epitaxial film exhibits intrinsic carrier transport properties, a high-quality epitaxial film of $Ca_3Co_4O_9$ may be an essential building block for this purpose. In addition, the film is also useful to clarify some of relevant TE properties of $Ca_3Co_4O_9$. For instance, the carrier mobility, which is very sensitive to the crystal quality, is evaluated accurately using thin films. However, epitaxial films with high crystal quality have not been prepared so far in spite of efforts using rf sputtering[12] and pulsed laser deposition techniques.[13]

$Ca_3Co_4O_9$ crystal is composed of an alternative stack of CdI_2-type CoO_2 layer and rock-salt-type Ca_2CoO_3 layer along the c axis.[14] Thus, one may consider that the crystallographic similarity of the CoO_2 layer to both $Ca_3Co_4O_9$ and M_xCoO_2 (M=Na, Li, Ca, and Sr) allows for the fabrication of the $Ca_3Co_4O_9$ epitaxial film by a "topotactic ion-exchange method" in which M ion in M_xCoO_2 epitaxial film is exchanged with Ca^{2+} ion through a suitable thermal annealing process.

Here we report the fabrication of high-quality epitaxial films of $Ca_3Co_4O_9$ by the topotactic ion-exchange method using a γ-Na_xCoO_2 epitaxial film, grown by a reactive solid-phase epitaxy[15] (R-SPE) method, as a precursor. The grown films thus exhibit high electrical conductivity resulting from large carrier mobility and reasonably large Seebeck coefficient, resulting in the thermoelectric power factor of 4.5×10^{-4} W m^{-1} K^{-2} at 300 K.

First, high-quality epitaxial films of γ-Na_xCoO_2 ($x\sim0.8$) were grown on the (0001) face of α-Al_2O_3 substrates by the R-SPE method, and they were used as a precursor for the following ion-exchange treatment. The details of the R-SPE for the preparation of γ-$Na_{0.8}CoO_2$ epitaxial films have been described elsewhere.[16] Then, the γ-$Na_{0.8}CoO_2$ film was heated together with $Ca(NO_3)_2$ powder at 300 °C for 5 h in air to exchange Na^+ ions with Ca^{2+} ions[17] (step 1 hereafter). After that, the film was washed with distilled water for several times to remove excess $Ca(NO_3)_2$ powder attached to the film. Finally, the ion-exchanged film was again heated with $Ca(OH)_2$ powder at 800 °C for 1 h in air to further incorporate Ca^{2+} ions into the film (step 2 hereafter).

a)Also at CREST, JST, 4-1-8 Honcho, Kawaguchi 332-0012, Japan.
b)Author to whom correspondence should be addressed; electronic mail: koumoto@apchem.nagoya-u.ac.jp

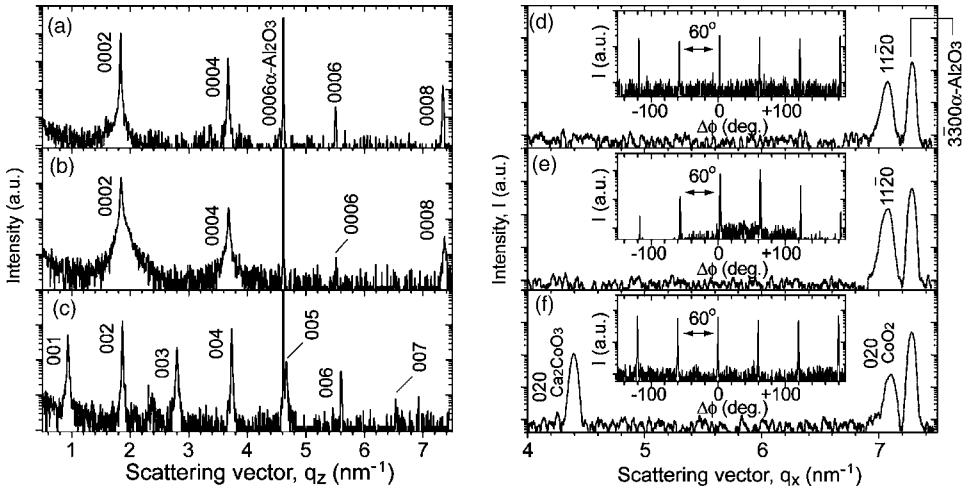

FIG. 1. HR-XRD patterns of [(a) and (d)] starting γ-$Na_{0.8}CoO_2$ epitaxial film grown on the (0001)-face of an α-Al_2O_3 substrate by R-SPE, [(b) and (e)] resultant γ-$Ca_{0.48}CoO_2$ film in step 1, and [(c) and (f)] resultant $Ca_3Co_4O_9$ film in step 2. (Left) Out-of-plane diffraction patterns of $2\theta/\omega$ synchronous scan. (Right) In-plane diffraction patterns of $2\theta\chi/\phi$ synchronous scan. In-plane rocking curves (ϕ scan) of (d) $\{11\bar{2}0_{\gamma\text{-}Na_{0.8}CoO_2}\}$, (e) $\{11\bar{2}0_{\gamma\text{-}Ca_{0.48}CoO_2}\}$, and (f) $\{020_{CoO_2}\}$ layers are also shown in the inset in each figure.

The crystalline quality, orientation, and thickness of the films were evaluated by high-resolution x-ray diffraction (HR-XRD) (ATX-G, Cu $K\alpha_1$, Rigaku Co.) measurements. The geometry of this x-ray diffractometer has been described in literature.[15,16] Figure 1 summarizes out-of-plane (left) and in-plane (right) XRD patterns of starting γ-$Na_{0.8}CoO_2$ epitaxial film [(a) and (d)], the resultant film in step 1 [(b) and (e)], and the resultant film in step 2 [(c) and (f)]. Only intense Bragg peaks for γ-$Na_{0.8}CoO_2$ $000l$ (l=even number) are seen in Fig. 1(a) together with the α-Al_2O_3 0006, indicating the highly c-axis-oriented film. The in-plane Bragg pattern (d) revealed that the γ-$Na_{0.8}CoO_2$ film is epitaxially grown on the α-Al_2O_3 substrate. Very similar Bragg peaks are observed after step 1 [(b) and (e)]. Out-of-plane peak position is slightly shifted to larger scattering vector side from those in Fig. 1(a). The chemical composition ratio of Ca:Co:Na in the film was evaluated to be 0.48:1.0:0.01 by x-ray fluorescence analysis. The lattice parameter of the film obtained from Fig. 1(b), c=1.0848 nm, agrees well with that of γ-$Ca_{0.35}CoO_2$ (c=1.0872 nm).[17] In-plane XRD patterns in step 1 were hardly changed in Figs. 1(d) and 1(e), indicating that CoO_2 layers were topotactically maintained. These observations clearly show that the ion exchange takes place through step 1 to change the film composition from γ-$Na_{0.8}CoO_2$ to γ-$Ca_{0.48}CoO_2$.

A dramatic change in the XRD pattern is observed after step 2 [(c) and (f)]. All the out-of-plane Bragg peaks were indexed as $00l$ (l=integer) $Ca_3Co_4O_9$ (Refs. 5, 9, and 14) in Fig. 1(c), and the lattice parameter c of the film was calculated to be 1.0708 nm, in reasonable agreement with that of $Ca_3Co_4O_9$ (c=1.0844 nm).[14] Furthermore, the formation of a $Ca_3Co_4O_9$ crystal is clearly observed in the in-plane XRD pattern (f), where intense two independent Bragg peaks at $q_x \sim 4.4$ and ~ 7.1 nm^{-1} were seen together with that for $3\bar{3}00$ α-Al_2O_3. The former peak corresponds to the 020 diffraction of a rock-salt-type Ca_2CoO_3 layer, indicating the formation of Ca_2CoO_3 layers, and the latter peak corresponds to that of a CdI_2-type CoO_2 layer, indicating that CoO_2 layers were topotactically maintained. The lattice parameters, b_{CoO_2} and $b_{Ca_2CoO_3}$, of the $Ca_3Co_4O_9$ film are 0.282 and 0.455 nm, respectively, agreeing well with reported values (b_{CoO_2}=0.2824 nm and $b_{Ca_2CoO_3}$=0.4558 nm).[14]

Through steps 1 and 2, sixfold symmetry was observed in each in-plane x-ray rocking curve of (d) $\{11\bar{2}0\}$ γ-$Na_{0.8}CoO_2$, (e) $\{11\bar{2}0\}$ γ-$Ca_{0.48}CoO_2$, and (f) $\{020\}$ CoO_2 layers in $Ca_3Co_4O_9$, indicating that the epitaxial layer remains unchanged during the topotactic ion-exchange process. The final epitaxial relationship was (001) $\times$[010]$Ca_3Co_4O_9$‖(0001)[$1\bar{1}00$]α-Al_2O_3.

Surface morphology of the $Ca_3Co_4O_9$ film was observed by an atomic force microscope (AFM) (SPI-3800N, S.I.I.) at room temperature. A stepped and terraced structure composed of several square-shaped domains (~ 1 μm^2) is clearly seen in a topographic AFM image (Fig. 2) of the film, reflecting the crystal symmetry of $Ca_3Co_4O_9$ (monoclinic). The step increment was approximately 3 nm, which is three times larger than that of the c-axis length of $Ca_3Co_4O_9$, suggesting that a step bunching occurred during the thermal annealing at 800 °C. From these results, we concluded that a high-quality $Ca_3Co_4O_9$ epitaxial film was fabricated by the topotactic ion-exchange method.

Electrical conductivity (σ), carrier concentration (n), and Hall mobility (μ_{Hall}) of the $Ca_3Co_4O_9$ epitaxial film were measured by a dc four-probe method in the van der Pauw configuration. The Seebeck coefficient (S) of the film was measured by a conventional steady state method. Figure 3(a)

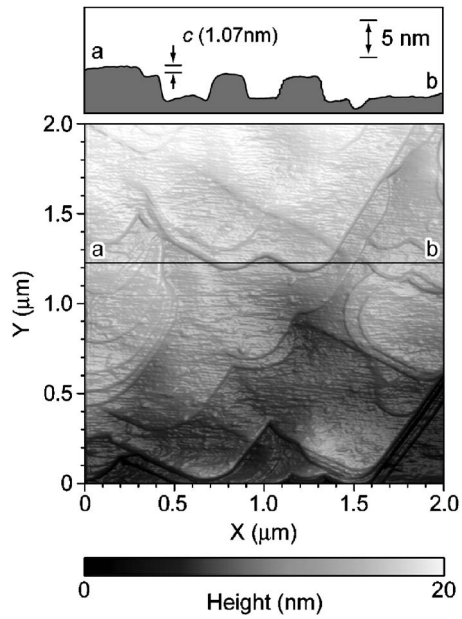

FIG. 2. Topographic AFM image of the $Ca_3Co_4O_9$ epitaxial film. Cross-sectional profile from (a) to (b) is shown on the top.

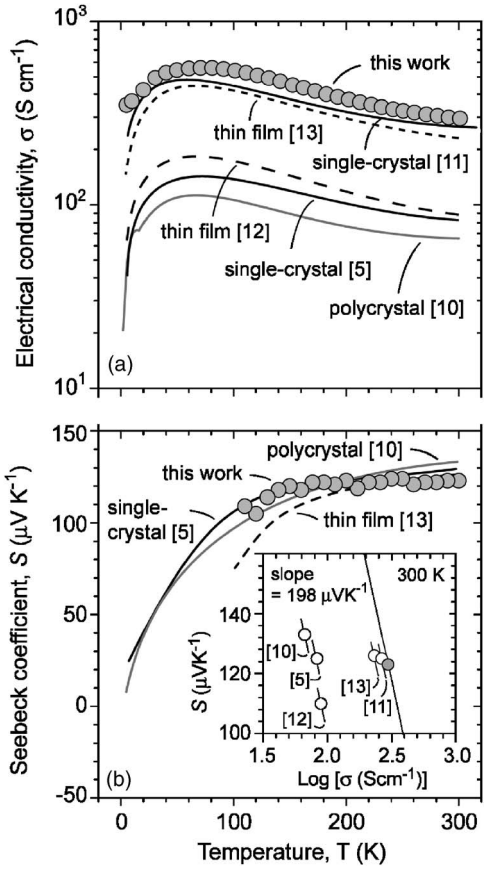

FIG. 3. Temperature dependence of (a) electrical conductivity σ and (b) Seebeck coefficient S for the $Ca_3Co_4O_9$ epitaxial film. Reported values of σ and S for $Ca_3Co_4O_9$ (Refs. 5 and 10–13) are also shown for comparison. (c) Jonker plot on $Ca_3Co_4O_9$ at 300 K. The solid line with a slope of theoretical S value ($-198\ \mu V\ K^{-1}$) is fitted to the data point of the present film.

shows temperature dependence of σ for the $Ca_3Co_4O_9$ epitaxial film (85 nm thick). The σ value was 2.95×10^2 S cm^{-1} at 300 K, which is larger than any other reported value in polycrystalline materials, thin films, and single crystals.[5,10–13] It gradually increases with decreasing temperature down to ~70 K. The values of n and μ_{Hall} of the $Ca_3Co_4O_9$ film were 1.2×10^{21} cm^{-3} and 1.5 cm^2 V^{-1} s^{-1}, respectively, at 300 K, suggesting that the large mobility could be responsible for the high electric conductivity. Figure 3(b) shows temperature dependence of S for the $Ca_3Co_4O_9$ epitaxial film, demonstrating a slight decrease with decreasing temperature, which is similar to the reported behavior.[5,10,13] Furthermore, the S value was evaluated to be $\sim +125\ \mu V\ K^{-1}$ at 300 K, reasonably agreeing with the reported values. The data point in terms of S and σ for the present epitaxial film is located on the right side of that of the bulk single crystal[11] in the Jonker plot,[18,19] as shown in the Fig. 3(b) inset, further confirming that the high conductivity is attributed to the enhanced carrier mobility. The thermoelectric power factor ($PF = S^2\sigma$) was evaluated to be 4.5×10^{-4} W m^{-1} K^{-2} at 300 K.

In summary, we have succeeded in fabricating high-quality epitaxial films of $Ca_3Co_4O_9$ by the topotactic ion-exchange method using the γ-$Na_{0.8}CoO_2$ epitaxial film on the (0001) face of the α-Al_2O_3 substrate as a precursor. The film exhibits an electrical conductivity of 2.95×10^2 S cm^{-1} and a Seebeck coefficient of $\sim +125\ \mu V\ K^{-1}$, leading to the thermoelectric power factor of 4.5×10^{-4} W m^{-1} K^{-2} at 300 K. The high conductivity, which is larger than any other value reported so far, is attributed to the larger carrier mobility resulting most likely from the high crystal quality of the films. Development of the $Ca_3Co_4O_9$ epitaxial film with a large PF value paves a way to further improve the TE performance of $Ca_3Co_4O_9$ through, for instance, the fabrication of a multi-quantum-well structure. Furthermore, the present high-quality epitaxial $Ca_3Co_4O_9$ film would play an essential role in understanding intrinsic TE properties of this material.

The authors thank Dr. Xiangyang Huang (CREST, JST) for a helpful discussion.

[1] I. Terasaki, Y. Sasago, and K. Uchinokura, Phys. Rev. B **56**, R12685 (1997).
[2] Y. Wang, N. S. Rogado, R. J. Cava, and N. P. Ong, Nature (London) **423**, 425 (2003).
[3] R. Ishikawa, Y. Ono, Y. Miyazaki, and T. Kajitani, Jpn. J. Appl. Phys., Part 2 **41**, L337 (2002).
[4] K. Sugiura, H. Ohta, K. Nomura, M. Hirano, H. Hosono, and K. Koumoto, Appl. Phys. Lett. **88**, 082109 (2006).
[5] A. C. Masset, C. Michel, A. Maignan, M. Hervieu, O. Toulemonde, F. Studer, and B. Raveau, Phys. Rev. B **62**, 166 (2000).
[6] M. Shikano and R. Funahashi, Appl. Phys. Lett. **82**, 1851 (2003).
[7] R. Funahashi, M. Mikami, S. Urata, M. Kitawaki, T. Kouuchi, and K. Mizuno, Meas. Sci. Technol. **16**, 70 (2005).
[8] G. Mahan, B. Sales, and J. Sharp, Phys. Today **50** (3), 42 (1997).
[9] H. Itahara, W.-S. Seo, S. Lee, H. Nozaki, T. Tani, and K. Koumoto, J. Am. Chem. Soc. **127**, 6367 (2005).
[10] Y. Miyazaki, K. Kudo, M. Akoshima, Y. Ono, Y. Koike, and T. Kajitani, Jpn. J. Appl. Phys., Part 2 **39**, L531 (2000).
[11] P. Limelette, V. Hardy, P. Auban-Senzier, D. Jérome, D. Flahaut, S. Hébert, R. Frésard, Ch. Simon, J. Noudem, and A. Maignan, Phys. Rev. B **71**, 233108 (2005).
[12] A. Sakai, T. Kanno, S. Yotsuhashi, A. Odagawa, and H. Adachi, Jpn. J. Appl. Phys., Part 2 **44**, L966 (2005).
[13] Y. F. Hu, W. D. Si, E. Sutter, and Q. Li, Appl. Phys. Lett. **86**, 082103 (2005).
[14] Y. Miyazaki, M. Onoda, T. Oku, M. Kikuchi, Y. Ishii, Y. Ono, Y. Morii, and T. Kajitani, J. Phys. Soc. Jpn. **71**, 491 (2002).
[15] H. Ohta, K. Nomura, M. Orita, M. Hirano, K. Ueda, T. Suzuki, Y. Ikuhara, and H. Hosono, Adv. Funct. Mater. **13**, 139 (2003).
[16] H. Ohta, S.-W. Kim, S. Ohta, K. Koumoto, M. Hirano, and H. Hosono, Cryst. Growth Des. **5**, 25 (2005).
[17] The topotactic route of an ion-exchange process to synthesize layered calcium cobalt oxides γ-Ca_xCoO_2 has been first reported in B. L. Cushing and J. B. Wiley, J. Solid State Chem. **141**, 385 (1998).
[18] G. H. Jonker, Philips Res. Rep. **23**, 131 (1968).
[19] T. Sekimoto, K. Kurosaki, H. Muta, and S. Yamanaka, Mater. Trans., JIM **46**, 1481 (2005).